Supplementary information
Oikawa, K. *et al.*

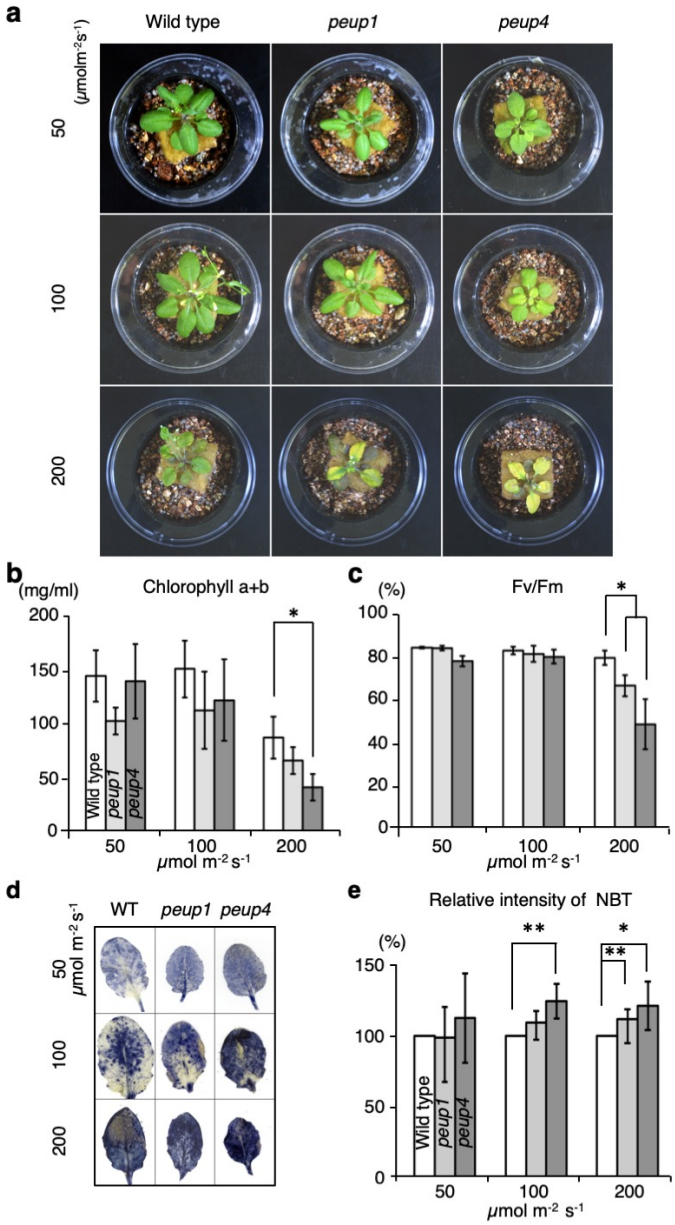

Supplementary Figure 1. Plant growth analysis of *peups* under different light intensities.

a, Plant growth of wild type (WT), *peup1*, and *peup4* under 50, 100, and 200 μmol m^{-2} s^{-1} light. **b**, **c,** Measurement of chlorophyll content (**b**) and photosynthetic efficiency (**c**) in the growth condition of (**a**). Three independent experiments were performed with three biological replicates. **d**, **e**, Nitroblue tetrazolium (NBT)-staining of representative leaf samples from WT, *peup1*, and *peup4* (**d**) and relative quantification of NBT intensity using totally 15 leaves (**e**). The error bars indicate mean ± standard deviation (five biological replicates), and asterisks indicate significant differences between WT and *peup4* in (**b**), between WT and *peup1* or *peup4* in (**c**), between WT and *peup4* under 100 μmol m^{-2} s^{-1} in (**e**), and between WT and *peup1* or *peup4* under 200 μmol m^{-2} s^{-1} in (**e**) (*P < 0.01, **P < 0.05, Student's t-test).

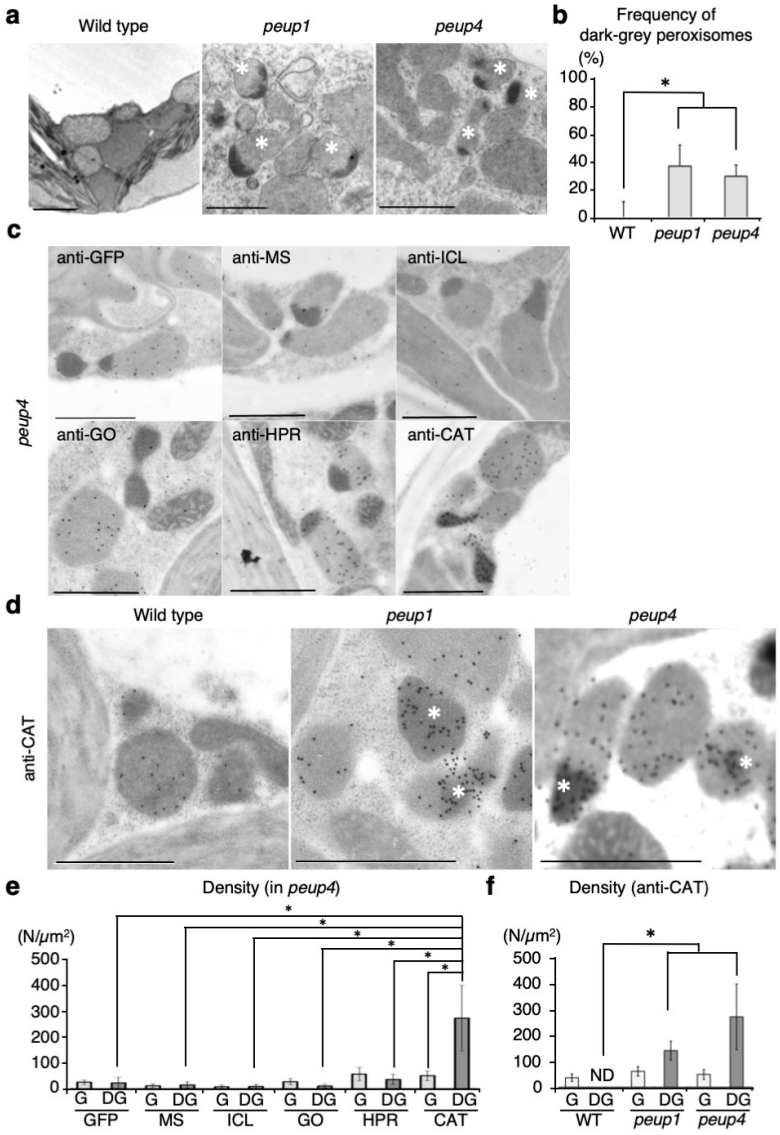

Supplementary Figure 2. Catalase accumulates in the high-density area of peroxisomes in *peup1* and *peup4*. **a,** Electron microscopic images of abnormal peroxisomes with high-density areas (dark-grey) (white asterisks) in *peup1* and *peup4* under normal light (100 μmol m^{-2} s^{-1}). **b**, Ratio of abnormal peroxisomes to total peroxisomes in the electron microscopic observation. Number of tested peroxisomes: wild type (WT) (n = 36), *peup1* (n = 134), and *peup4* (n = 183). The error bars indicate mean ± standard deviation (five different sections), and asterisks indicate significant differences between WT and *peup1* or *peup4* (*P < 0.01, Student's t-test). **c**, Immunoelectron microscopy analyses performed using antibodies against GFP, malate synthase (MS), isocitrate lyase (ICL), glycolate oxidase (GO), hydroxypyruvate reductase (HPR), and catalase (CAT) in GFP-PTS1 expressing plants. Scale bars, 1 μm. **d**, Enlarged images show that anti-CAT gold particles are highly accumulated in high-density areas (dark-grey) of peroxisomes in *peup1* and *peup4* (white asterisks), but not in WT. **e**, Density of antibodies detected in grey (G) or dark-grey (DG) peroxisomes in (**c**). Number of tested peroxisomes: GFP (n = 32), MS (n = 22), ICL (n = 15), GO (n = 37), HPR (n = 35), CAT (n = 30). The error bars indicate mean ± standard deviation, and asterisks indicate significant differences between density of each antibodies detected in DG in *peup4* (*P < 0.01, Student's t-test). **f**, Density of antibody against CAT in grey (G) or dark-grey (DG) peroxisomes of GFP-PTS1, *peup1*, and *pup4*. Number of tested DG: GFP-PTS1 (n = 7), *peup1* (n = 14), and *pup4* (n = 23). The error bars indicate mean ± standard deviation (five different sections), and asterisks indicate significant differences of density of anti-CAT gold particles between WT and *peup1* or *peup4* (*P < 0.01, Student's t-test).

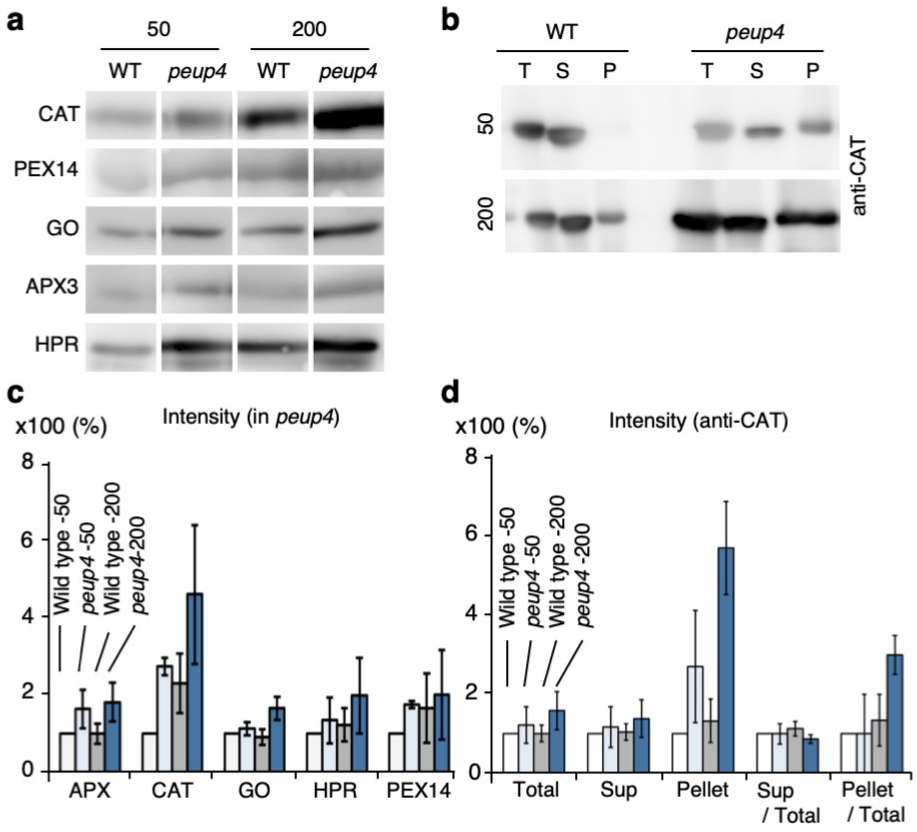

Supplementary Figure 3. High accumulation of catalase in *peup4* under light.

a, Immunoblotting analysis of the total extract from 50 or 200 µmol m^{-2} s^{-1} light-adapted wild type (WT) and *peup4* by using antibodies against catalase (CAT), peroxin 14 (PEX14), glycolate oxidase (GO), ascorbate peroxidase (APX3), and hydroxypyruvate reductase (HPR). **b,** Immunoblotting analysis of catalase in each fraction (total: T, supernatant: S, and pellet: P). **c**, **d**, Relative quantification of signal intensity corresponding to (**a**) and (**b**). The graph shows a summary of three biological replicates.

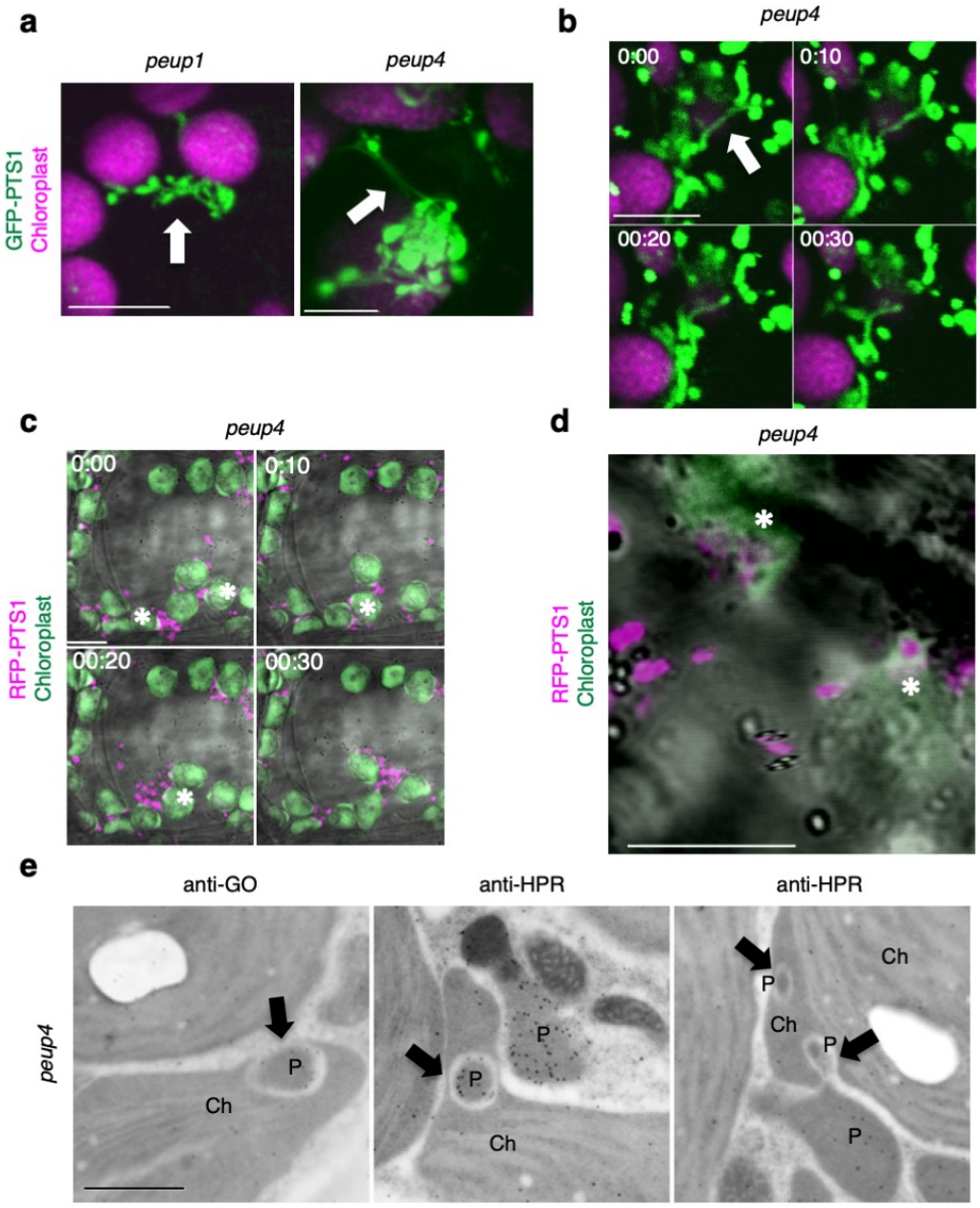

Supplementary Figure 4. Peroxules and stromules are generated in *peup4*.
a, Peroxisomes (GFP-PTS1, green) and chloroplasts (autofluorescence, magenta) in 100 µmol m^{-2} s^{-1} light-adapted *peup1* and *peup4*. **b**, Time-lapse images of peroxules extended from peroxisome aggregation in *peup4* obtained every 10 s. White arrows indicate peroxules in (**a**) and (**b**). **c**, Time-lapse images of engulfment (white asterisks) of peroxisomes (RFP-PTS1, magenta) by chloroplast membranes (autofluorescence, green) in *peup4* obtained every 10 s. **d**, An enlarged image shows peroxisomes in chloroplast membranes (white asterisks). Scale bars in (**a**–**d**), 10 µm. **e**, EM images of peroxisomes and chloroplasts in *peup4*. Arrows (black) indicate the engulfment of peroxisomes (P) by chloroplasts (Ch). Peroxisomes are identified using anti- glycolate oxidase (GO) or anti-hydroxypyruvate reductase (HPR) antibody. Scale bars, 1 µm.

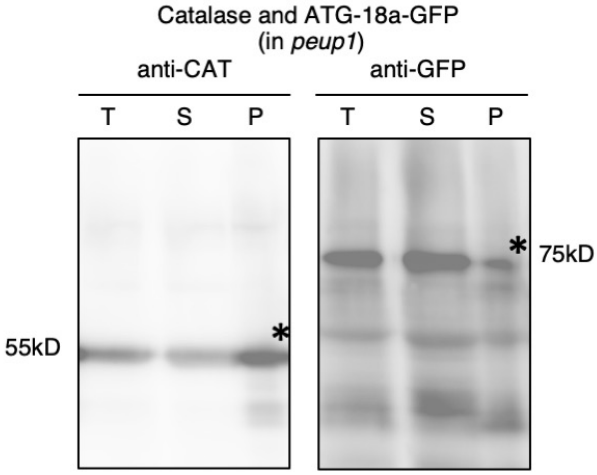

Supplementary Figure 5. Co-localisation of ATG18a-GFP and peroxisome in the pellet fraction.
Immunoblotting analysis of catalase (left) and ATG18a-GFP (right) in each fraction (total: T, supernatant: S, and pellet: P). Signals corresponding to CAT and ATG18a-GFP are indicated by black asterisks.

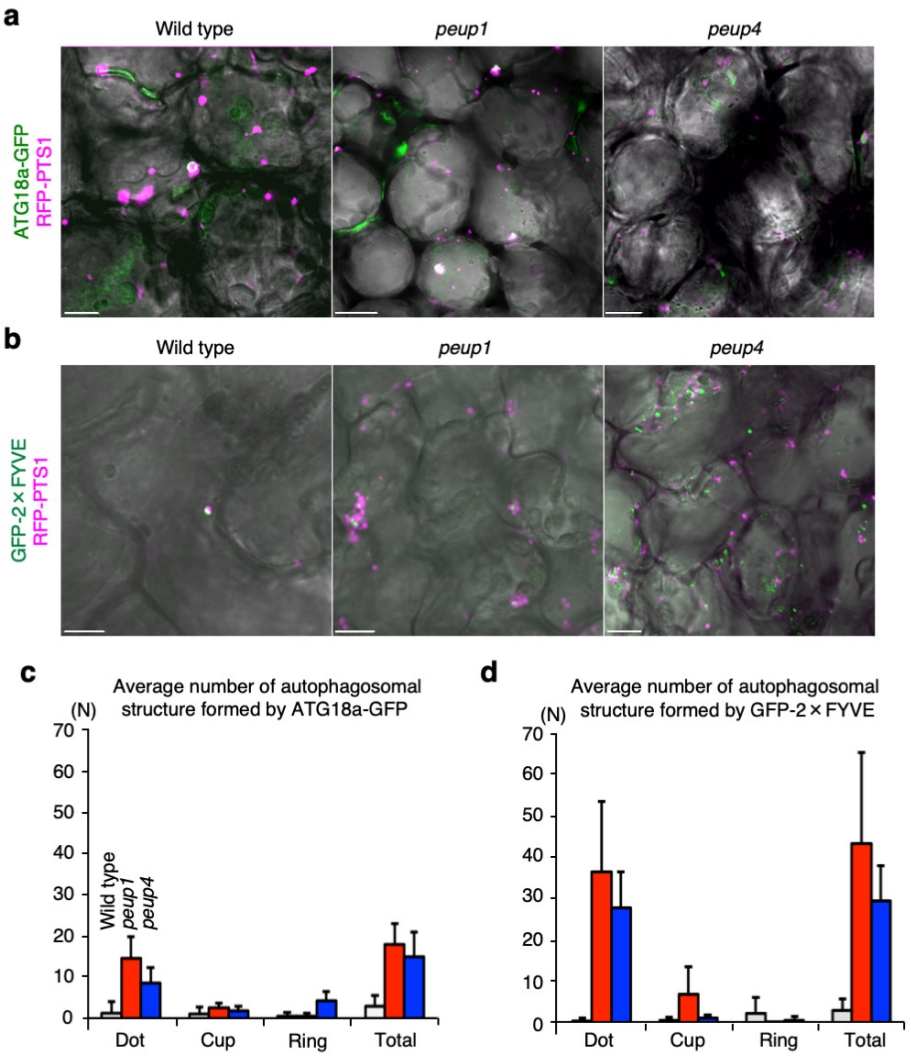

Supplementary Figure 6. Quantification of ATG18a-GFP and GFP-2×FYVE targeting peroxisomes in *peup1* and *peup4*.

a, **b**, Representative images used for statistical analysis of peroxisomes in wild type, *peup1*, and *peup4* targeted by ATG18a-GFP (**a**) or GFP-2×FYVE (**b**). Scale bars, 10 μm. **c**, **d**, Number of ATG18-GFP or GFP-2×FYVE structures on peroxisomes; the structures are categorised into three types: dot, cup, and ring. The data are taken from ten cells and shown as the density at 100 × 100 μm^2. Number of three patterns for ATG18a-GFP (**c**) or GFP-2×FYVE (**d**) in (**Supplementary Table 1**) are shown as a graph from every 10 images.

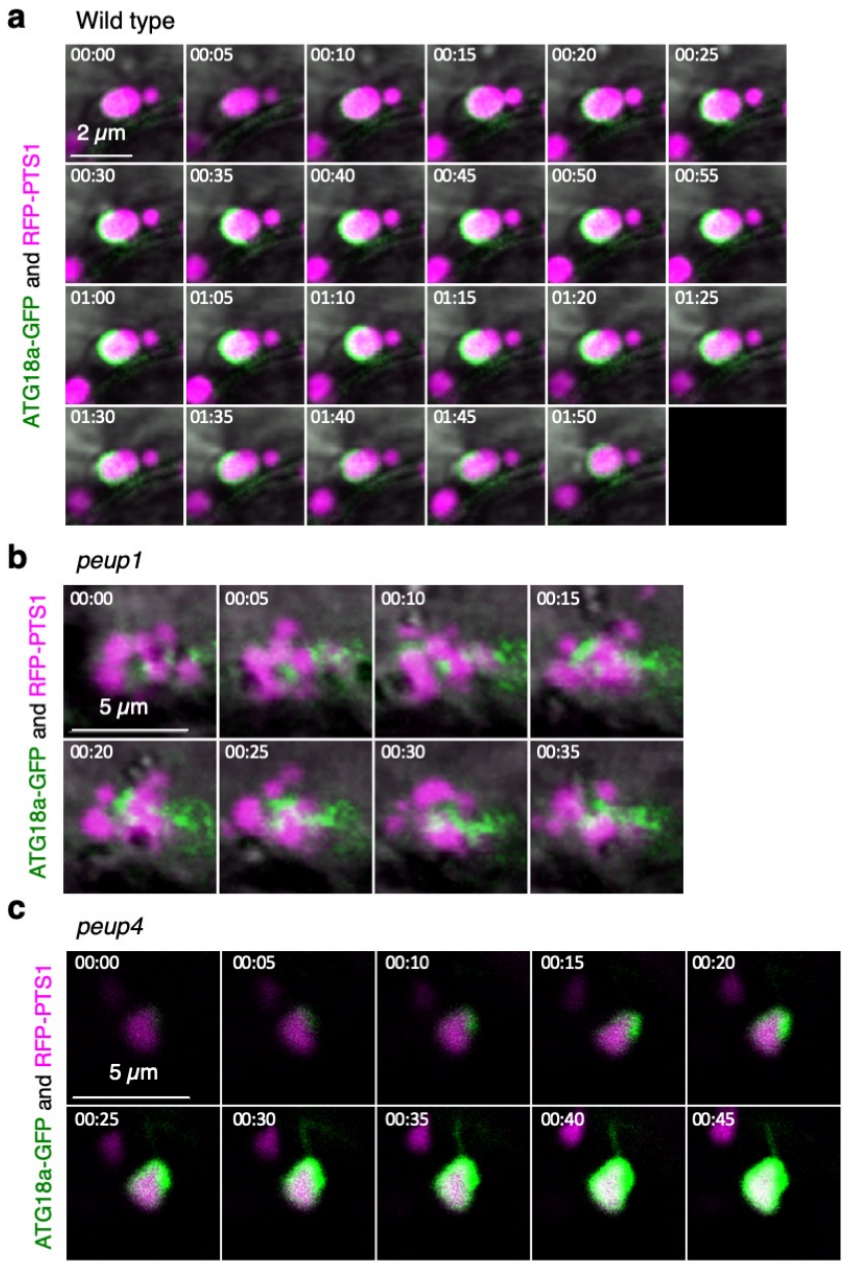

Supplementary Figure 7. Time-lapse analyses of ATG18a-GFP in wild type, *peup1*, and *peup4*.
a–c, Time-lapse images of peroxisome (magenta) and ATG18a-GFP (green) in wild type (**a**), *peup1* (**b**), and *peup4* (**c**) were obtained every 5 s. ATG18a-GFP surrounds the peroxisome in wild type (**a**) and *peup4* (**c**), but not in *peup1* (**b**).

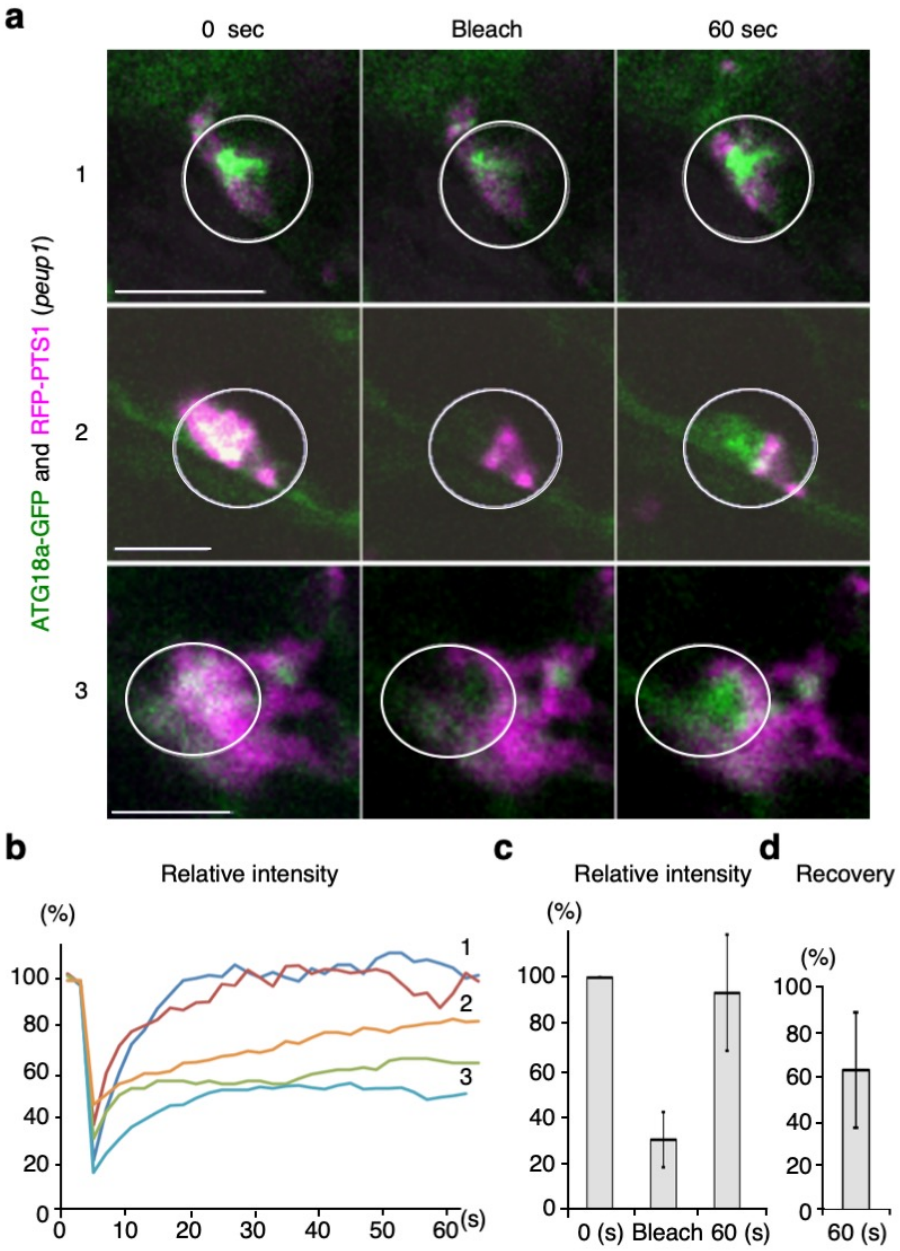

Supplementary Figure 8. FRAP analysis for ATG18a-GFP targeting peroxisome aggregation in *peup1*.
a, Three representative images (1–3) of fluorescence recovery after photobleaching (FRAP) analysis of ATG18a-GFP in *peup1*. The images shown are before (0 sec), just after (Bleach), and after 60 seconds of bleaching. Scale bars, 5 μm. **b**, Kinetic changes of GFP fluorescence. Five individuals obtained by FRAP analyses are shown in different colours. The numbers 1–3 correspond to those in (**a**). **c**, Relative GFP fluorescence in the five FRAP analyses in (**b**). **d**, Fluorescence recovery of GFP after bleaching is calculated from (**c**).

a

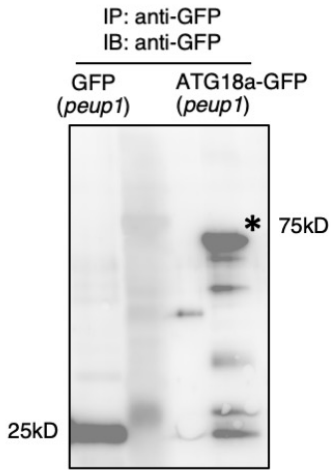

b

Number of proteins in data bases and immunoprecipitation, and recovery ratio.

	PPDB [a]	SUBA4 [a]	IP [b]	IP/PPDB (%) [c]	IP/SUBA4 (%) [c]
Chloroplast	2433	3281	15	0.62	0.46
Mitochondrion	567	2170	2	0.35	0.09
Peroxisome	228	292	8	3.51	2.74

[a] Number of proteins in the organelles indicated in the data bases (PPDB and SUBA4). [b] Number of proteins identified in immunoprecipitation of ATG18a-GFP (IP). [c] Recovery ratio calculated from the numbers.

Supplementary Figure 9. Mass spectral analysis to identify ATG18a-GFP interacting proteins.
a, Immunoblot of GFP with the samples for MS analysis. **b**, Number of proteins in databases and immunoprecipitation, and recovery ratio. Asterisk indicates the band of ATG18a-GFP.

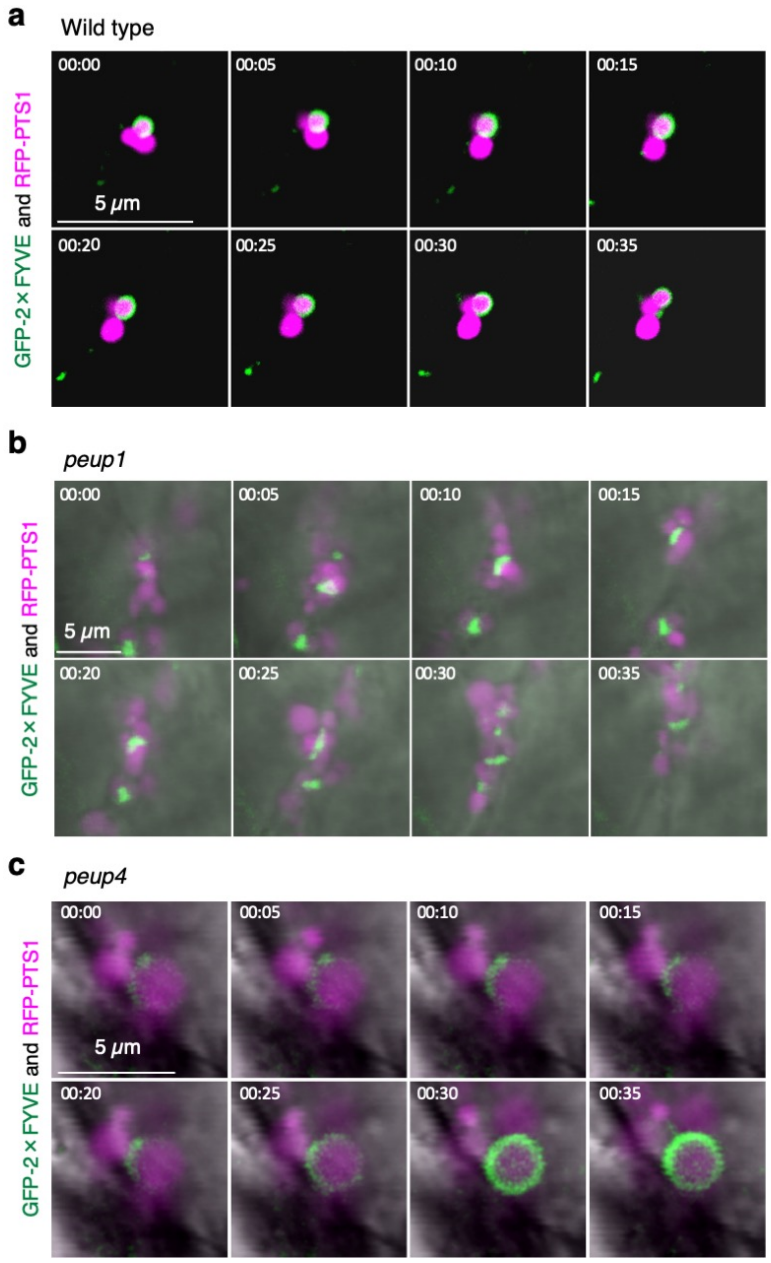

Supplementary Figure 10. Time-lapse analyses of GFP-2xFYVE in wild type, *peup1*, and *peup4*.
a–c, Time-lapse images of peroxisome (RFP-PTS1, magenta) and GFP-2×FYVE (green) in wild type (**a**), *peup1* (**b**), and *peup4* (**c**) were obtained every 5 seconds. GFP-2×FYVE surrounds the peroxisome in wild type (**a**) and *peup4* (**c**) but not in *peup1* (**b**)

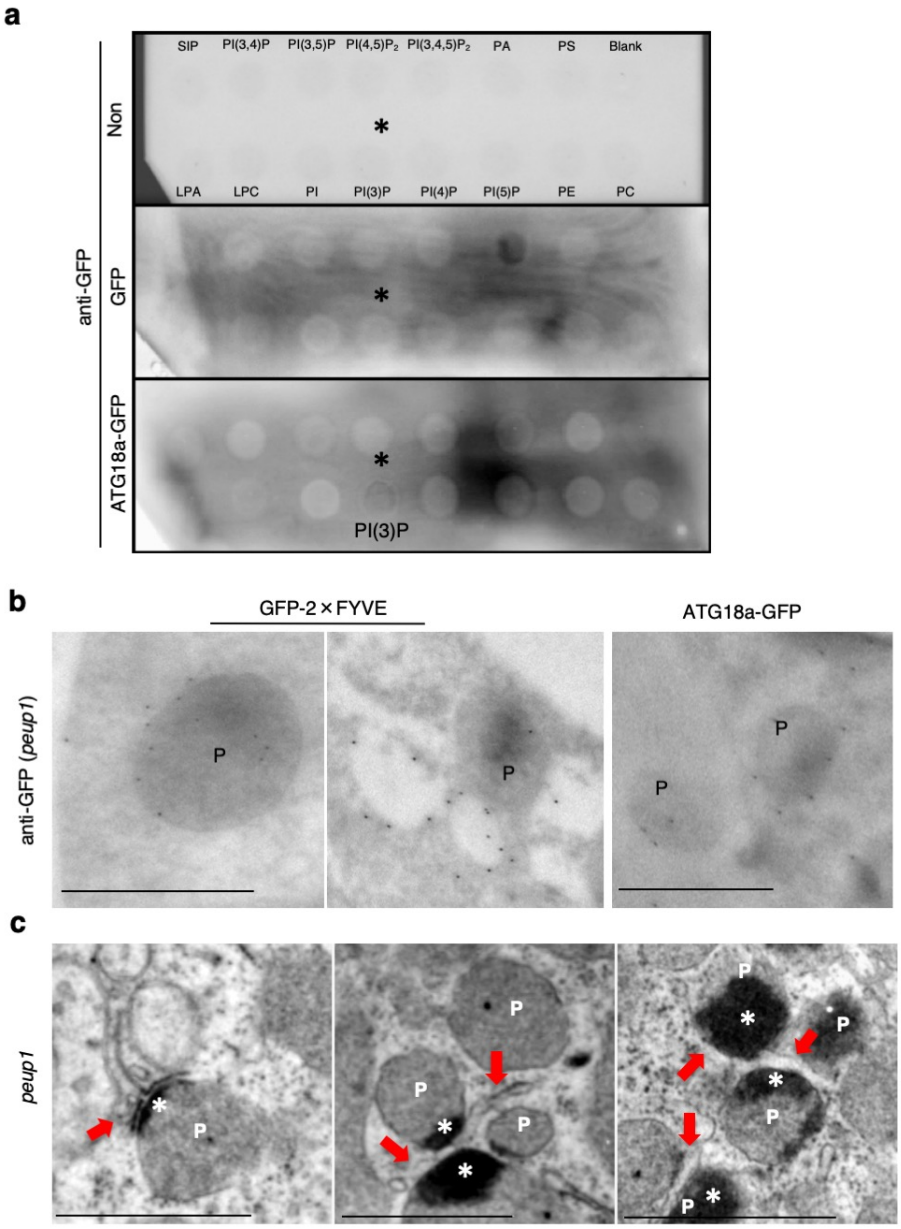

Supplementary Figure 11. Lipid-binding test and EM analyses show that ATG18a-GFP targets PtdIns3P formed on peroxisomes in *peup1*.

a, Binding of ATG18a-GFP to PtdIns3P (PI(3)P; black asterisks) on membrane lipid strips. The bound ATG18a-GFP was detected on immunoblot with anti-GFP antibody. Each spot displays Sphingosine 1-phosphate: S1P, PtdIns(3,4)P_2: PI(3,4)P_2, PtdIns(3,5)P_2: PI(3,5)P_2, PtdIns(4,5)P2: PI(4,5)P_2, PtdIns(3,4,5)P_3: PI(3,4,5)P_3, Phosphatidic acid: PA, PtdSer: PS, Lysophosphatidic acid: LPA, Lysophosphocholine: LPC, PtdIns4P: PI(4)P, PtdIns5P: PI(5)P, PtdEtn; PE, and PedCho: PC. **b**, Immunoelectron microscopy analysis of *peup1* expressing *GFP-2×FYVE* (left and middle) and *ATG18a-GFP* (right) using antibody against GFP. Black dots show GFP-2×FYVE and ATG18a-GFP on peroxisomes (P), which contain high-density regions. Note that GFP-2×FYVE localises on both peroxisomes and PAS-like structures formed around peroxisomes, whereas ATG18a-GFP localises on the periphery of peroxisomes. Scale bars, 1 µm. **c**, ER and the PAS-like structures (red arrows) are close to the high-dense area (white asterisks) in peroxisomes (P) of *peup1*. Scale bars, 2 µm.

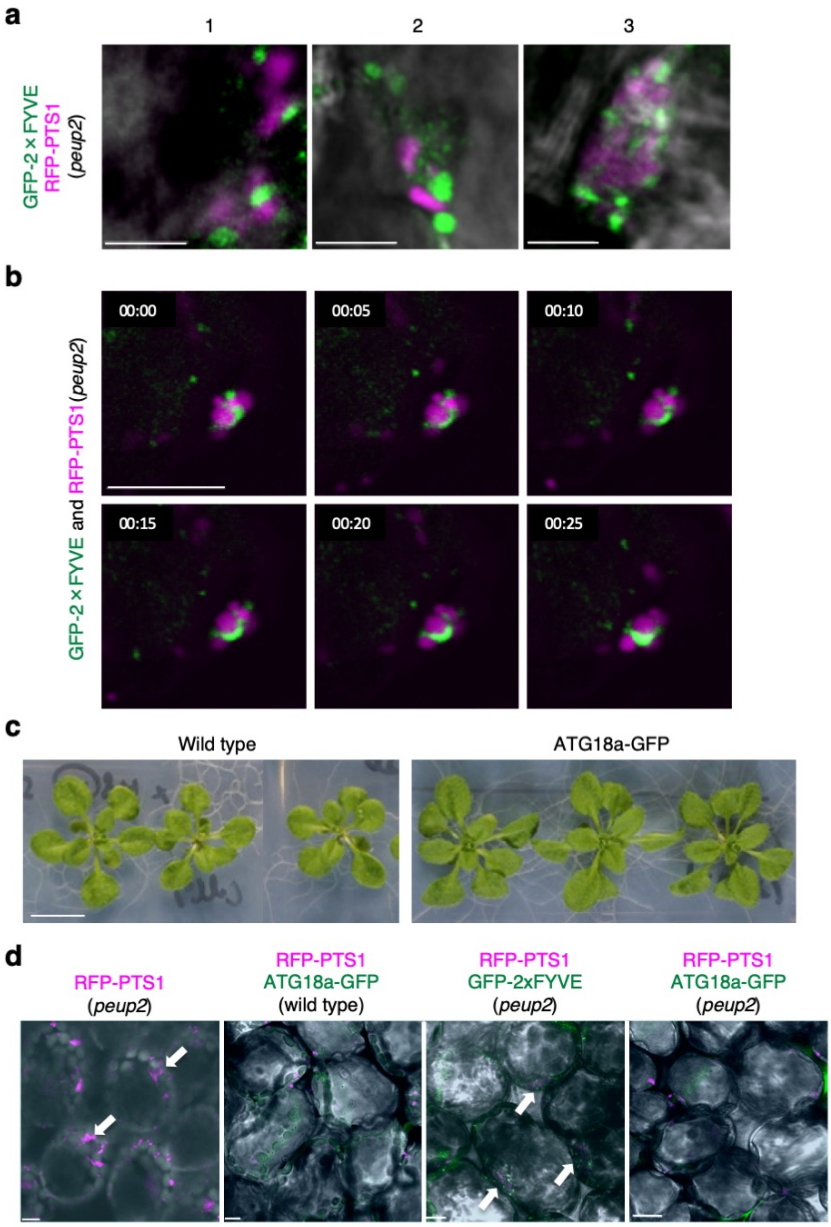

Supplementary Figure 12. ATG18a-GFP complements the mutant phenotype of *peup2/atg18a*.
a, Three different images of peroxisomes (RFP-PTS1, magenta) and GFP-2×FYVE (green) in *peup2*. Scale bars, 5 µm. **b**, Time-lapse images of peroxisomes and GFP-2×FYVE in *peup2* taken every 5 seconds. Note that GFP-2×FYVE targeted peroxisome aggregations in ATG18a-deficient *peup2*. Scale bar, 5 µm. **c** Plant growth of wild type (Col-0) and the transgenic plants expressing *ATG18a-GFP*. Scale bar, 1 cm. **d**, Merged images show peroxisomes (RFP-PTS1, magenta), ATG18a-GFP or GFP-2×FYVE (green), and chloroplasts (grey globular structures) in wild type or *peup2*. Peroxisome aggregations are shown as white arrows. Note that *peup2* expressing *ATG18a-GFP* shows similar peroxisomes as that in wild type. Scale bars, 10 µm.

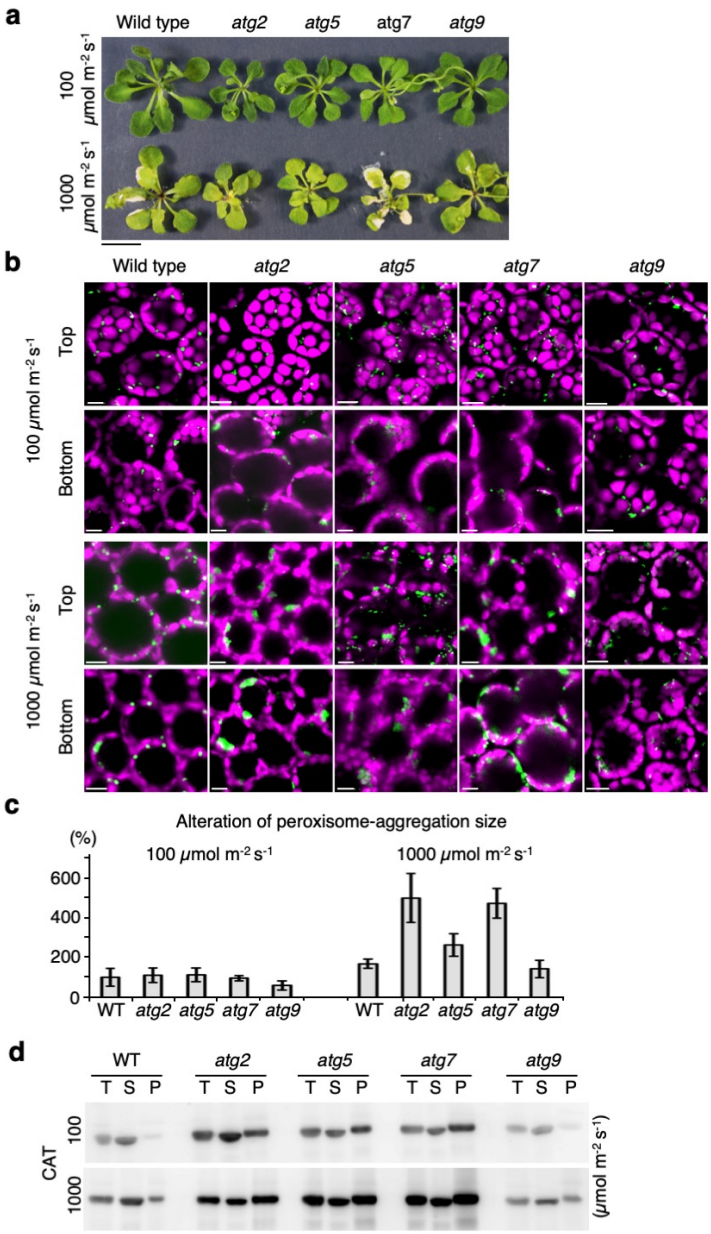

Supplementary Figure 13. Effect of high-intensity light on leaf damage, induction of large peroxisome aggregates, and accumulation of catalase in autophagy mutants.

A, Plant growth analysis of wild type and *atg2, atg5, atg7*, and *atg9* under normal (100) and high-intensity light (1000 μmol m^{-2} s^{-1}). Scale bar, 1 cm. **b**, Peroxisomes (GFP-PTS1, green) and chloroplasts (autofluorescence, magenta) at the region from top to middle (Top) and from middle to bottom (Bottom) of leaf mesophyll cells of wild type, *atg2, atg5, atg7*, and *atg9* under normal (100) and high-intensity light (1000 μmol m^{-2} s^{-1}). Scale bars, 10 μm. Note that large aggregates of peroxisome are formed in *atg2* and *atg7* under high-intensity light. **c**, Relative size of peroxisome aggregation in (**b**) is calculated. Sixteen peroxisome aggregations are tested. The error bars indicate mean ± standard deviation (five biological replicates), and asterisks indicate significant differences of size of peroxisomes between wild type and *atg2* or *atg7* (*$P < 0.01$, Student's *t*-test). **d**, Immunoblot analysis of catalase (CAT) in total (T), supernatant (S), and pellets (P) of leaf extract.

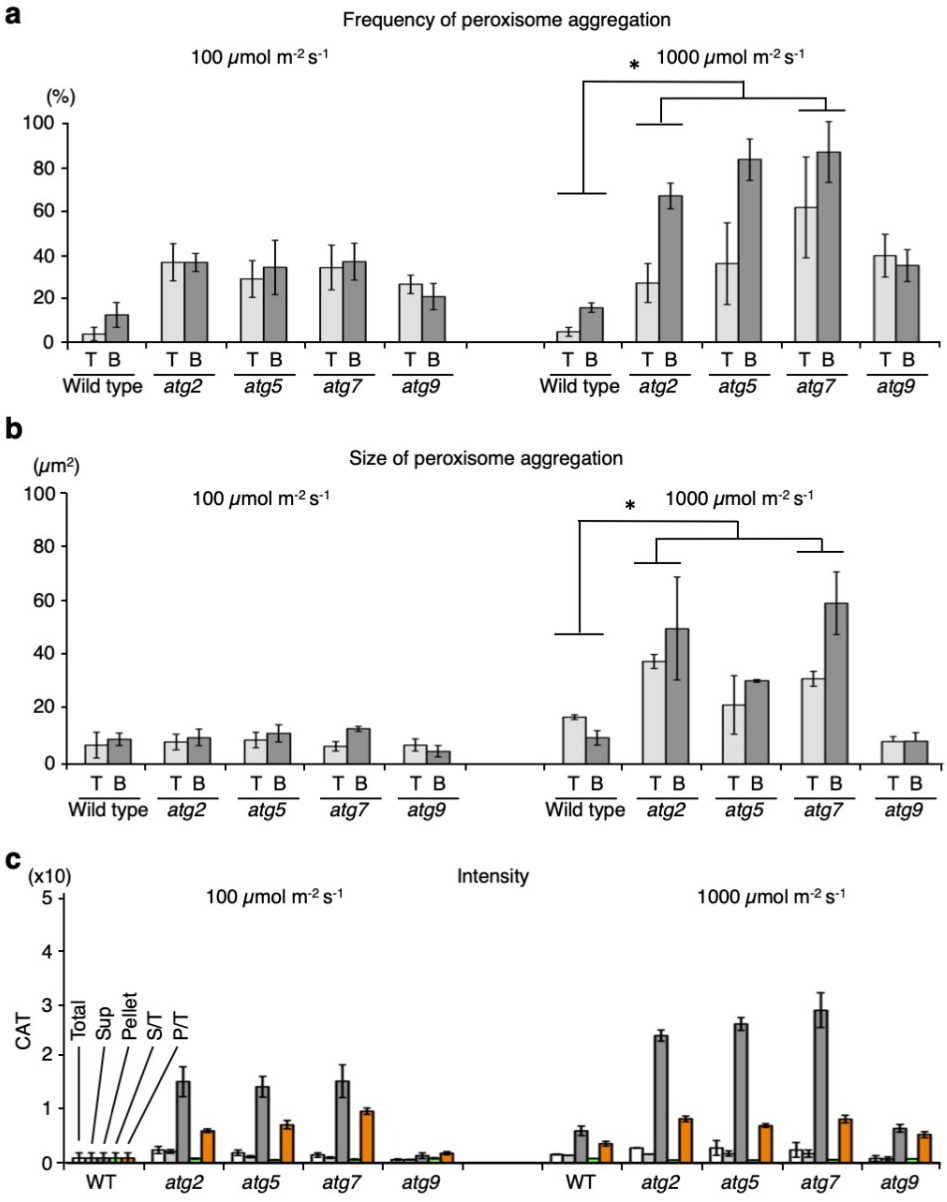

Supplementary Figure 14. Quantification of large peroxisome aggregates and catalase accumulation in wild type, *atg2*, *atg5*, *atg7*, and *atg9*.

a, **b**, Frequency of cells containing peroxisome aggregates (**a**) and size of peroxisome aggregation (**b**) in wild type (WT), *atg2*, *atg5*, *atg7*, and *atg9* under normal (100 μmol m^{-2} s^{-1}) and high-intensity light (1000 μmol m^{-2} s^{-1}). T, top to middle region; B, middle to bottom region of mesophyll cells. More than 100 cells were tested in (**a**). Each tested number for normal light in (**b**): WT top ($n = 6$), WT bottom ($n = 28$), *atg2* top ($n = 50$), *atg2* bottom ($n = 63$), *atg5* top ($n = 43$), *atg5* bottom ($n = 65$), *atg7* top ($n = 83$), *atg7* bottom ($n = 90$), *atg9* top ($n = 22$), *atg9* bottom ($n = 18$); for high-intensity light in (**b**): WT top ($n = 19$), WT bottom ($n = 48$), *atg2* top ($n = 52$), *atg2* bottom ($n = 55$), *atg5* top ($n = 45$), *atg5* bottom ($n = 76$), *atg7* top ($n = 42$), *atg7* bottom ($n = 49$), *atg9* top ($n = 40$), *atg9* bottom ($n = 41$). The error bars indicate mean ± standard deviation (three biological replicates), and asterisks indicate significant differences of size of peroxisomes between WT and *atg2* or *atg7* (*$P < 0.01$, Student's *t*-test). **c**, Signal intensity of immunoblotting analysis using anti-CAT antibody in **Supplementary Figure 13d** was measured using Dot Blot Analysis in ImageJ. The results of each fraction and supernatant or pellet per total are shown as graphs. The experiments were repeated at least three times.

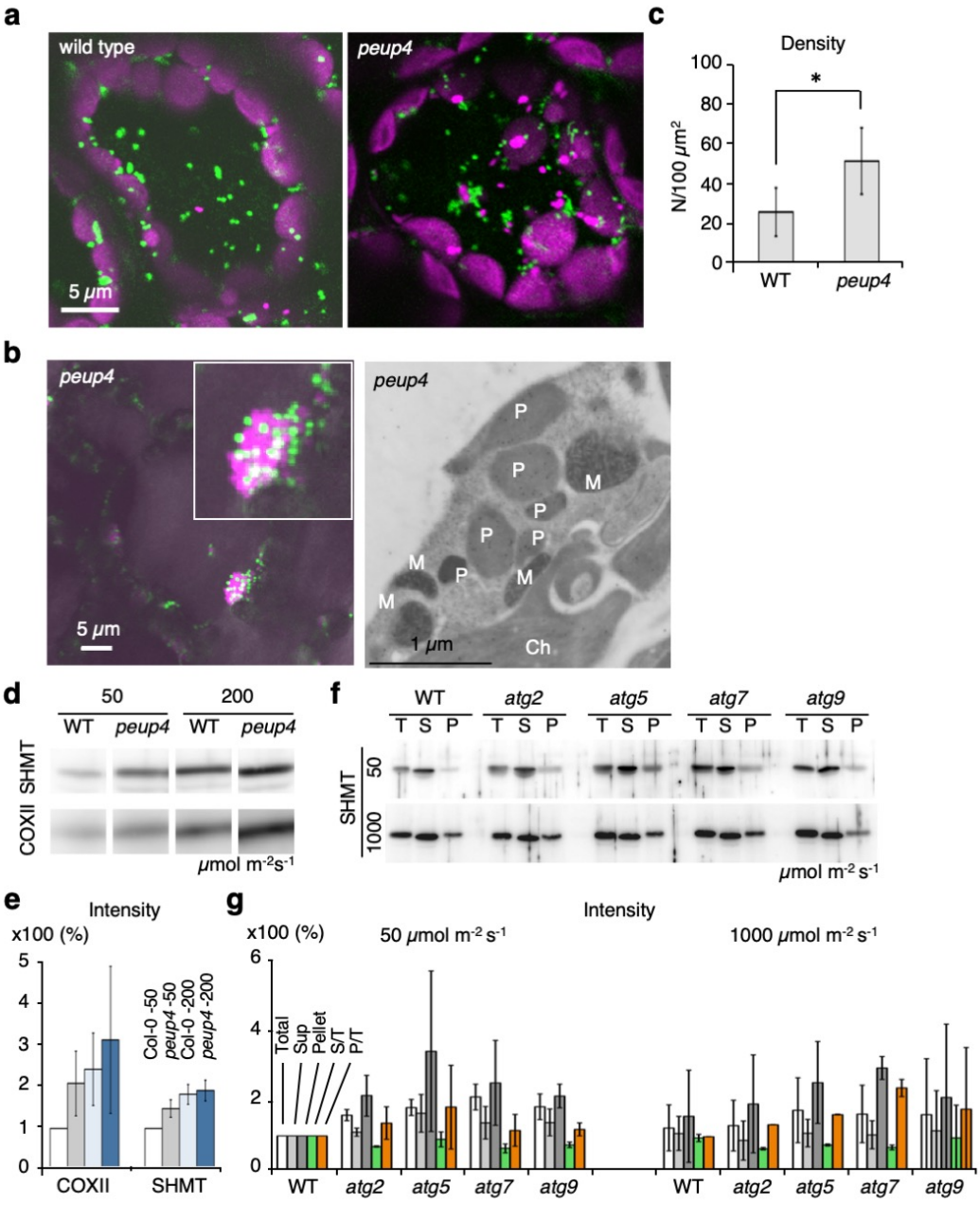

Supplementary Figure 15. Mitochondrial degradation in *peup4* is slightly impaired in light.
a, Mitochondria (γATPase-GFP, green), peroxisomes (RFP-PTS1, magenta), and chloroplasts (autofluorescence, magenta) in leaf mesophyll cells of wild type and *peup4* under 200 μmol m^{-2} s^{-1} light. Mitochondria are observed in the peroxisome aggregate contacting chloroplast in the fluorescence image (left) and electron microscope image (right). P; peroxisome, M; mitochondrion, and Ch; chloroplast. **c**, Density of mitochondria. The data are collected from more than 100 cells in CLSM images. **d**, **e**, Immunoblotting analysis of leaf extraction of *peup4* adapted to 50 and 200 μmol m^{-2} s^{-1} light using anti-serine hydroxymethyltransferase (SHMT) and anti-cytochrome c oxidase 2 (COXII) antibody (**d**) and measurement of signal intensity (**e**). **f**, **g**, Immunoblotting analysis of leaf fractionation (total: T, supernatant: S, and pellet: P) extracted from *atg* mutants adapted to 50 and 1000 μmol m^{-2} s^{-1} light using anti-SHMT antibody (**f**) and measurement of signal intensity (**g**).

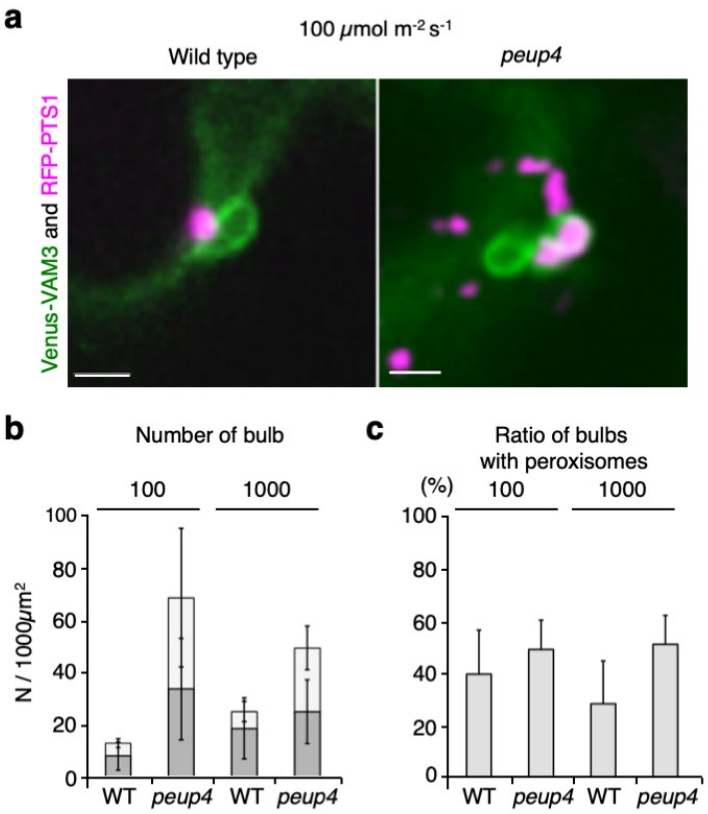

Supplementary Figure 16. Vacuole structure around peroxisomes in *peup4*.

a, Bulb structures generated from vacuolar membranes (Venus-VAM3, green) around peroxisomes (RFP-PTS1, magenta) in wild type and *peup4*. Scale bars, 1 μm. **b**, **c**, Density of the bulb structures with (white box) or without (grey box) peroxisomes in 1 mm^2 (**b**) and the frequency of the bulbs with peroxisomes (**c**) under normal (100 μmol m^{-2} s^{-1}) and high-intensity (1000 μmol m^{-2} s^{-1}) light-adapted leaves of wild type and *peup4*.

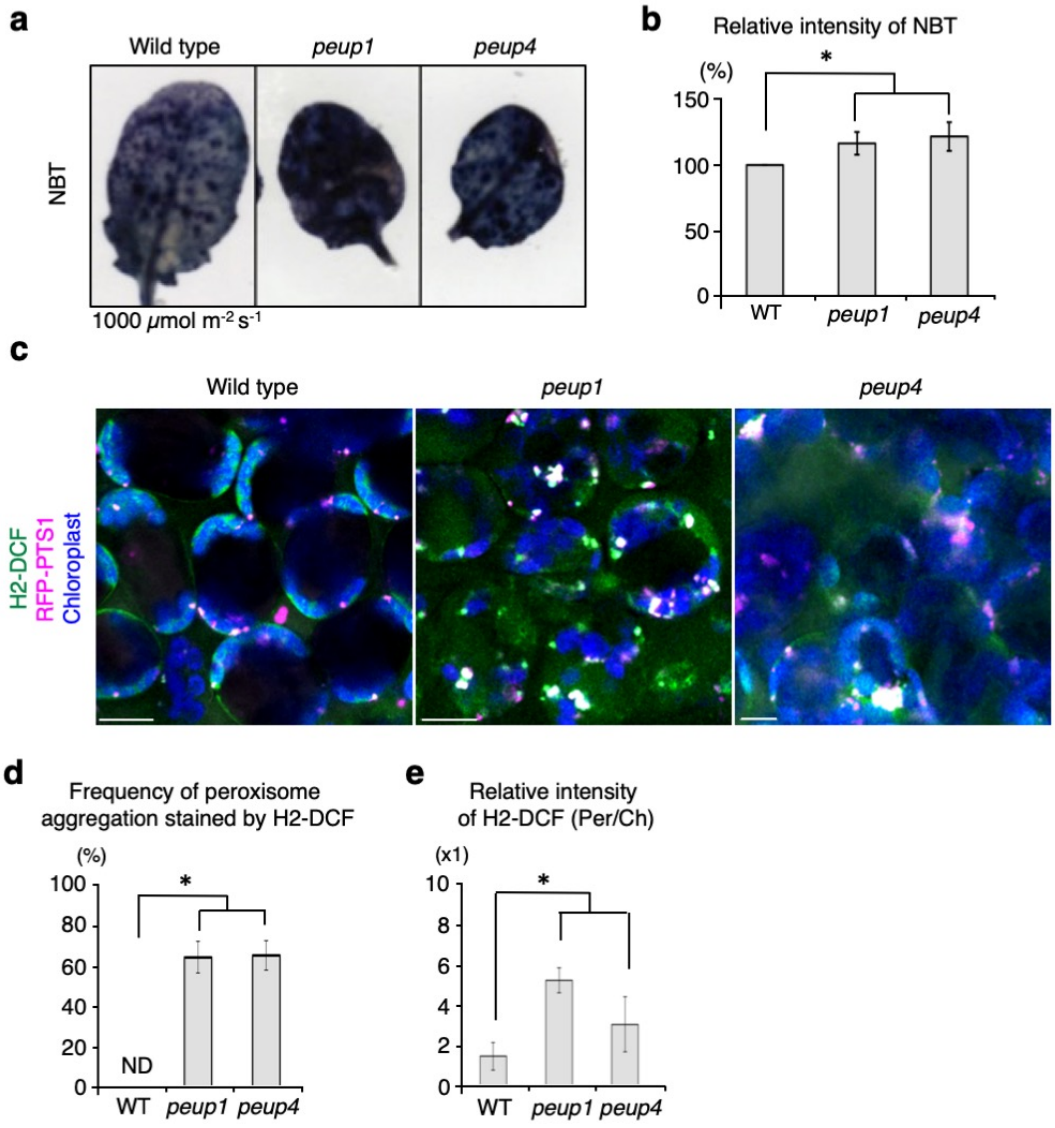

Supplementary Figure 17. High accumulation of ROS in the peroxisomes of *peup1* and *peup4* in high-intensity light.

a, Nitroblue tetrazolium (NBT)-stained leaves of wild type (WT), *peup1*, and *peup4* after exposure to high-intensity light (1000 μmol m^{-2} s^{-1}) for 16 h. **b**, Relative NBT intensity in leaves of WT, *peup1*, and *peup4*. The error bars indicate mean ± standard deviation (three biological replicates), and black asterisks represent significant differences between WT and *peup1* or *peup4* (*P < 0.01 Student's *t*-test). Fifteen leaves were tested. **c**, Detection of ROS in leaf mesophyll cells of wild type, *peup1*, and *peup4* stained with H2-DCF after exposure to high-intensity light for 16 h. Note that most peroxisomes (RFP-PTS1, magenta) in a large aggregation and small parts of the chloroplast (autofluorescence, blue) are stained with DCF (green). Scale bars, 10 μm. **d**, Frequency of peroxisome aggregates stained with H2-DCF to total peroxisome aggregates. Number of aggregations: WT (n = 11), *peup1* (n = 89), and *peup4* (n = 49). **e**, Relative intensity of H2-DCF in peroxisomes to that in chloroplasts. Number of cells: WT (n = 151), *peup1* (n = 140), and *peup4* (n = 135). The error bars indicate mean ± standard deviation (five biological replicates), and black asterisks represent significant differences between WT and *peup1* or *peup4* (*P < 0.01, Student's *t*-test) in (**d**, **e**).

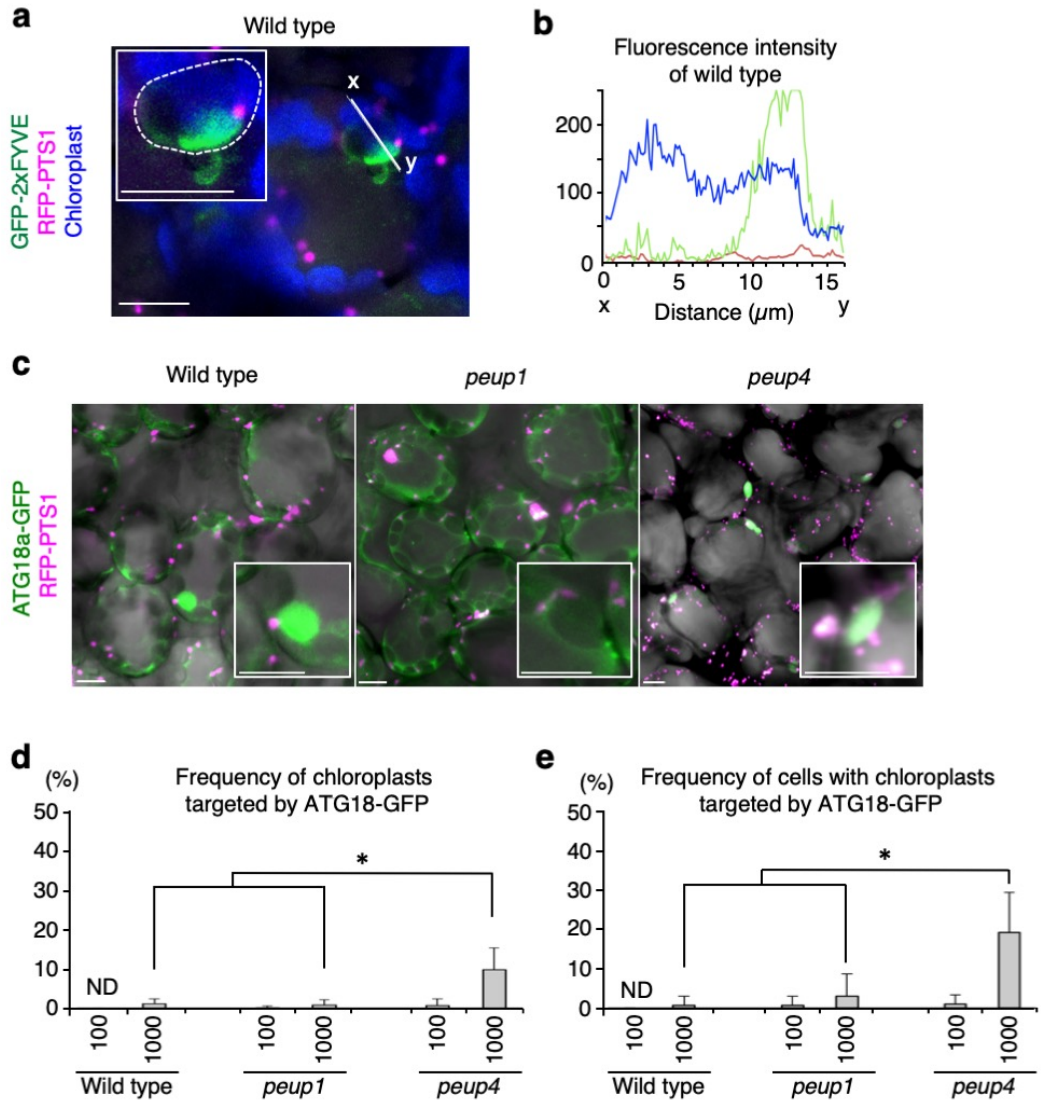

Supplementary Figure 18. Accumulation of ROS in the chloroplasts of *peup1* and *peup4* in high-intensity light.

a, Chloroplasts (blue) targeted by GFP-2×FYVE (green) in a leaf mesophyll cell of wild type expressing *RFP-PTS1*. A chloroplast targeted by GFP-2×FYVE is surrounded by white-broken line. **b**, Plot profile of fluorescence on line x-y across a chloroplast (blue line) surrounded by GFP-2×FYVE (green line) in the image (lower panel) in (**a**). Scale bar, 5 μm. **c,** Chloroplasts (grey globular structures) targeted by ATG18a-GFP (green) in leaf mesophyll cells of wild type, *peup1*, and *peup4* expressing *RFP-PTS1*. Scale bars, 5 μm. **d**, Frequency of chloroplasts targeted by ATG18a-GFP to total number of chloroplasts (*P < 0.01, Student's t-test). Number of tested chloroplasts: WT, normal light (n = 649); WT, high-intensity light (n = 628); *peup1*, normal light (n = 651); *peup1*, high-intensity light (n = 605); *peup4*, normal light (n = 812); and *peup4*, high-intensity light (n = 479). **e,** Cells containing ATG18a-GFP-targeted chloroplasts to total number of cells. Number of tested cells: wild type, normal light (n = 110); wild type, high-intensity light (n = 280); *peup1*, normal light (n = 190); *peup1*, high-intensity light (n = 190); *peup4*, normal light (n = 234); and *peup4*, high-intensity light (n = 298). The error bars indicate mean ± standard deviation (five biological replicates), and asterisks represent significant differences between wild type and *peup1* or *peup4* (*P < 0.01, Student's t-test) in (**d, e**).

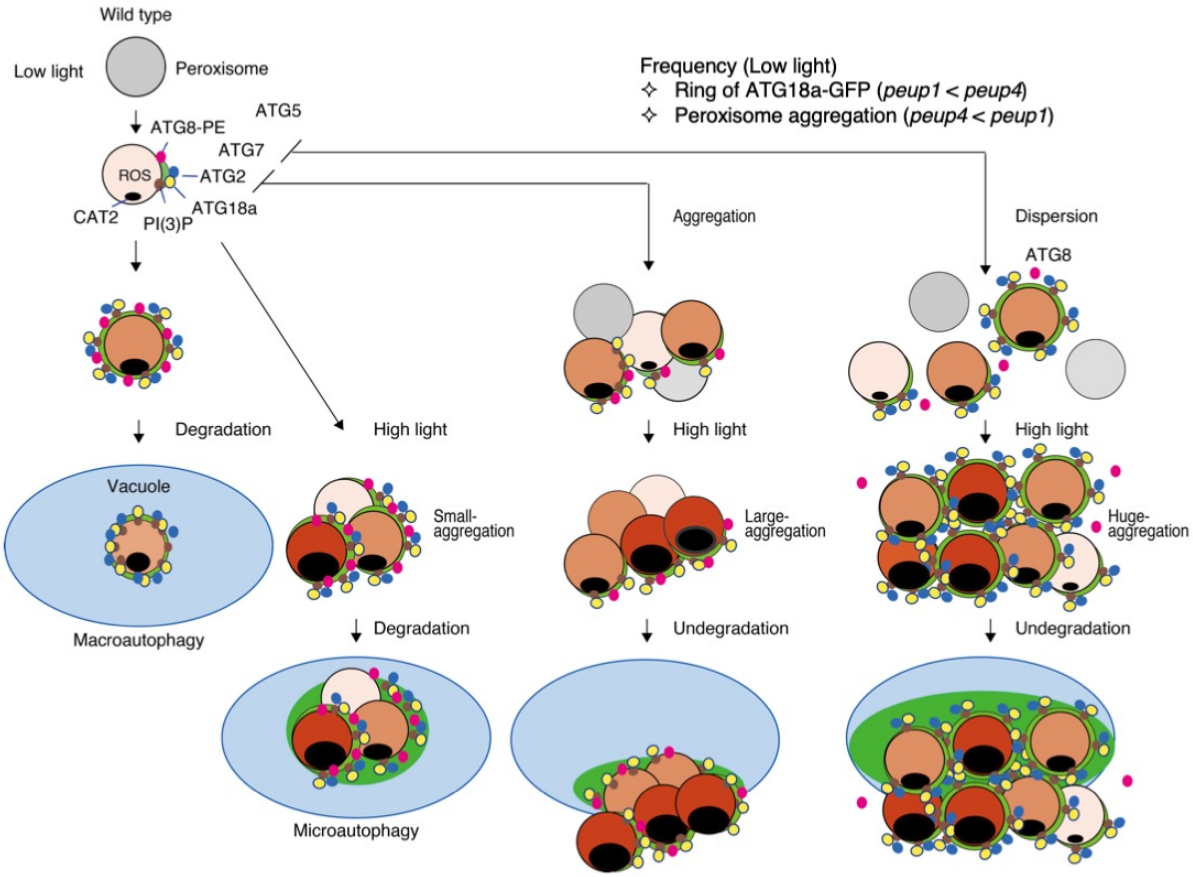

Supplementary Figure 19. Model for processing pexophagosome formation in *peup1* and *peup4*.
Peroxisomes in *peup4* are enveloped by both GFP-2×FYVE and ATG18a-GFP, whereas peroxisomes in *peup1* are not. This difference may generate different phenotypes of peroxisome aggregation between *peup1* and *peup4*: peroxisomes in *peup1/atg2* form strong aggregates, whereas those in *peup4/atg7* disperse and show weak aggregation under normal light (see Fig.1). ATG18a and ATG2 are essential for the initiation of pexophagosome formation. ATG7 is involved in the maturation of pexophagosomes by synthesising the ATG8-PE conjugate on the membrane of pexophagosomes, which are transported to vacuoles for degradation[11,14]. Both *peup1* and *peup4* form a large aggregate of peroxisomes with high accumulation of catalase and ROS under high-intensity light, which is preferentially targeted by GFP-2×FYVE and ATG18a-GFP (see Figs. 4-6 and Supplementary Figs. 13,14). In *peup4*, but not in *peup1*, the peroxisome aggregation surrounded by ATG18a-GFP is enveloped as a large globular structure by a vacuolar membrane similar to that in macropexophagy (see Fig. 5); however, it cannot be degraded without ATG8-PE[11,14].

Supplementary Table 1.

Number of ATG18-GFP or GFP-2×FYVE structures on peroxisomes; the structures are categorised into three types: dot, cup, and ring. The data are taken from ten cells and shown as the density at 100 × 100 μm^2.

ATG18-GFP 10000 (μm^2)

	Dot	Cup	Ring	Total	Number
Wild type	1.37	1.13	0.56	3.06	10
peup1	14.87	2.65	0.61	18.14	10
peup4	8.73	2.02	4.40	15.15	10

GFP-2×FYVE 10000 (μm^2)

	Dot	Cup	Ring	Total	Number
Wild type	0.43	0.51	2.21	3.15	10
peup1	36.28	6.85	0.05	43.19	10
peup4	27.74	1.08	0.59	29.40	10

Supplementary Table 2.

List of identified proteins by MS analysis for immunoparticipation with ATG18a-GFP (*peup1*)

	prot_acc	prot_desc	significant score (a)	molecular mass (b)	count of spectrum matches (c)	significant spectrum matches (d)
PM (Cell wall)	AT3G16530.1	| Symbols: | Legume lectin family protein | chr3:5624586-5625416 REVERSE LENGTH=276	204	30547	10	8
	AT3G15356.1	| Symbols: | Legume lectin family protein | chr3:5174603-5175418 REVERSE LENGTH=271	79	29788	4	4
	AT3G53420.1	| Symbols: PIP2A, PIP2, PIP2;1 | plasma membrane intrinsic protein 2A | chr3:19803906-19805454 REVERSE LENGTH=287	43	30683	2	2
	AT5G20630.1	| Symbols: GLP3, GLP3A, GLP3B, ATGER3, GER3 | germin 3 | chr5:6975315-6975950 REVERSE LENGTH=211	37	21993	1	1
	AT2G01210.1	| Symbols: | Leucine-rich repeat protein kinase family protein | chr2:119509-121734 REVERSE LENGTH=716	35	79284	23	1
	AT1G01620.1	| Symbols: PIP1C, TMP-B, PIP1;3 | plasma membrane intrinsic protein 1C | chr1:225986-227176 REVERSE LENGTH=286	23	30841	1	1
Cytoplasm	AT5G09810.1	| Symbols: ACT7 | actin 7 | chr5:3052809-3054220 FORWARD LENGTH=377	121	41937	4	4
	AT3G46520.1	| Symbols: ACT12 | actin-12 | chr3:17128567-17129981 FORWARD LENGTH=377	72	41996	4	3
	AT5G14740.1	| Symbols: CA2, CA18, BETA CA2 | carbonic anhydrase 2 | chr5:4758257-4762382 FORWARD LENGTH=331	69	37105	1	1
	AT1G23410.1	| Symbols: | Ribosomal protein S27a / Ubiquitin family protein | chr1:8314940-8315410 FORWARD LENGTH=156	35	17889	2	1
	AT2G02930.1	| Symbols: ATGSTF3, GST16, GSTF3 | glutathione S-transferase F3 | chr2:851348-852106 REVERSE LENGTH=212	34	24106	1	1
	AT3G19050.1	| Symbols: POK2 | phragmoplast orienting kinesin 2 | chr3:6578047-6590106 FORWARD LENGTH=2771	31	317659	36	1
	AT1G10890.1	| Symbols: | unknown protein; FUNCTIONS IN: molecular_function unknown; INVOLVED IN: biological_process unknown; LOCATED IN: chloroplast; EXPRESSED IN: petal, flower, leaf; EXPRESSED DURING: LP.04 four leaves visible, 4 anthesis, petal differentiation and expansion stage; BEST Arabidopsis thaliana protein match is: unknown protein (TAIR:AT5G13340.1); Has 11769 Blast hits to 8435 proteins in 698 species: Archae - 22; Bacteria - 971; Metazoa - 5937; Fungi - 1065; Plants - 592; Viruses - 101; Other Eukaryotes - 3081 (source: NCBI BLink). | chr1:3628081-3630545 FORWARD LENGTH=288	22	34607	2	1
	AT5G57950.1	| Symbols: | 26S proteasome regulatory subunit, putative | chr5:23460765-23462128 FORWARD LENGTH=227	22	24361	17	1
	AT4G29770.1	| Symbols: | Target of trans acting-siR480/255. | chr4:14576371-14577465 FORWARD LENGTH=277	21	31737	8	2
Vacuole	AT3G58810.1	| Symbols: MTPA2, ATMTPA2, MTP3, ATMTP3 | metal tolerance protein A2 | chr3:21750551-21751849 FORWARD LENGTH=432	15	47928	4	2
Unknown	AT1G04090.1	| Symbols: | Plant protein of unknown function (DUF946) | chr1:1057225-1059247 FORWARD LENGTH=572	36	64955	1	1
	AT1G67050.1	| Symbols: | unknown protein; BEST Arabidopsis thaliana protein match is: unknown protein (TAIR:AT5G38320.1); Has 617 Blast hits to 318 proteins in 80 species: Archae - 0; Bacteria - 16; Metazoa - 141; Fungi - 62; Plants - 128; Viruses - 2; Other E	34	28909	9	4
	AT5G50530.1	| Symbols: | CBS / octicosapeptide/Phox/Bemp1 (PB1) domains-containing protein | chr5:20571876-20574922 REVERSE LENGTH=548	32	60060	4	3
	AT1G49780.1	| Symbols: PUB26 | plant U-box 26 | chr1:18429024-18430289 REVERSE LENGTH=421	26	46561	7	1
HSP	AT5G02500.1	| Symbols: HSC70-1, HSP70-1, AT-HSC70-1, HSC70 | heat shock cognate protein 70-1 | chr5:554055-556334 REVERSE LENGTH=651	437	71712	22	19
	AT3G09440.1	| Symbols: | Heat shock protein 70 (Hsp 70) family protein | chr3:2903434-2905632 REVERSE LENGTH=649	329	71559	19	16
	AT5G02490.1	| Symbols: | Heat shock protein 70 (Hsp 70) family protein | chr5:550296-552565 REVERSE LENGTH=653	325	71741	19	16
	AT5G28540.1	| Symbols: BIP1 | heat shock protein 70 (Hsp 70) family protein | chr5:10540665-10543274 REVERSE LENGTH=669	108	73869	10	5
	AT4G24280.1	| Symbols: cpHsc70-1 | chloroplast heat shock protein 70-1 | chr4:12590094-12593437 FORWARD LENGTH=718	52	76575	3	2
Proteosome	AT1G23410.1	| Symbols: | Ribosomal protein S27a / Ubiquitin family protein | chr1:8314940-8315410 FORWARD LENGTH=156	35	17889	2	1
	AT1G49780.1	| Symbols: PUB26 | plant U-box 26 | chr1:18429024-18430289 REVERSE LENGTH=421	26	46561	7	1
	AT5G57950.1	| Symbols: | 26S proteasome regulatory subunit, putative | chr5:23460765-23462128 FORWARD LENGTH=227	22	24361	17	1
Lipid(membrane)	AT3G15730.1	| Symbols: PLDALPHA1, PLD | phospholipase D alpha 1 | chr3:5330835-5333474 FORWARD LENGTH=810	166	92246	15	9
	AT1G07920.1	| Symbols: | GTP binding Elongation factor Tu family protein | chr1:2455559-2457001 FORWARD LENGTH=449	98	49813	5	4
	AT3G06650.1	| Symbols: ACLB-1 | ATP-citrate lyase B-1 | chr3:2079247-2082633 REVERSE LENGTH=608	34	66342	1	1

Autophagy

	prot_acc	prot_desc	significant score (a)	molecular mass (b)	count of spectrum matches (c)	significant spectrum matches (d)
Nucleus	AT3G49490.1	| Symbols: | unknown protein; Has 722 Blast hits to 186 proteins in 64 species: Archae - 0; Bacteria - 30; Metazoa - 72; Fungi - 48; Plants - 38; Viruses - 0; Other Eukaryotes - 534 (source: NCBI BLink). | chr3:18344926-18348648 REVERSE LENGTH=953	289	106078	10	10
	AT1G63160.1	| Symbols: RFC2 | replication factor C 2 | chr1:23422068-23423771 REVERSE LENGTH=333	64	37066	22	5
	AT4G39680.1	| Symbols: | SAP domain-containing protein | chr4:18414604-18416938 REVERSE LENGTH=633	39	69514	2	2
	AT2G25000.1	| Symbols: WRKY60, ATWRKY60 | WRKY DNA-binding protein 60 | chr2:10629812-10631095 FORWARD LENGTH=271	26	30730	1	1
	AT4G37080.1	| Symbols: | Protein of unknown function, DUF547 | chr4:17474205-17476716 FORWARD LENGTH=597	22	67930	14	2
	AT1G53090.1	| Symbols: SPA4 | SPA1-related 4 | chr1:19783748-19786690 FORWARD LENGTH=794	21	90099	25	1
	AT1G20400.1	| Symbols: | Protein of unknown function (DUF1204) | chr1:7072192-7075838 REVERSE LENGTH=944	21	107183	1	1
	AT5G10710.1	| Symbols: | INVOLVED IN: chromosome segregation, cell division; LOCATED IN: chromosome, centromeric region, nucleus; EXPRESSED IN: 23 plant structures; EXPRESSED DURING: 13 growth stages; CONTAINS InterPro DOMAIN/s: Centromere protein Cenp-O (Inte	20	36454	1	1
Chloroplast	ATCG00490.1	| Symbols: RBCL | ribulose-bisphosphate carboxylases | chrC:54958-56397 FORWARD LENGTH=479	218	53435	9	7
	AT2G39730.1	| Symbols: RCA | rubisco activase | chr2:16570951-16573345 REVERSE LENGTH=474	157	52347	3	3
	AT3G18890.1	| Symbols: | NAD(P)-binding Rossmann-fold superfamily protein | chr3:6511169-6514729 FORWARD LENGTH=641(Tic62)	58	68642	4	2
	AT4G24280.1	| Symbols: cpHsc70-1 | chloroplast heat shock protein 70-1 | chr4:12590094-12593437 FORWARD LENGTH=718	52	76575	3	2
	AT3G50820.1	| Symbols: PSBO2, PSBO-2, OEC33 | photosystem II subunit O-2 | chr3:18891008-18892311 REVERSE LENGTH=331	39	35226	1	1
	AT1G29910.1	| Symbols: CAB3, AB180, LHCB1.2 | chlorophyll A/B binding protein 3 | chr1:10472443-10473246 REVERSE LENGTH=267	37	28266	3	2
	AT4G10340.1	| Symbols: LHCB5 | light harvesting complex of photosystem II 5 | chr4:6408200-6409496 FORWARD LENGTH=280	35	30195	2	2
	AT5G38420.1	| Symbols: | Ribulose bisphosphate carboxylase (small chain) family protein | chr5:15381203-15381978 REVERSE LENGTH=181	25	20622	3	1
	AT1G67090.1	| Symbols: RBCS1A | ribulose bisphosphate carboxylase small chain 1A | chr1:25048465-25049249 REVERSE LENGTH=180	25	20488	2	1
	ATCG00280.1	| Symbols: PSBC | photosystem II reaction center protein C | chrC:33720-35141 FORWARD LENGTH=473	25	52063	1	1
	ATCG00340.1	| Symbols: PSAB | Photosystem I, PsaA/PsaB protein | chrC:37375-39579 REVERSE LENGTH=734	23	82537	1	1
	AT2G45180.1	| Symbols: | Bifunctional inhibitor/lipid-transfer protein/seed storage 2S albumin superfamily protein | chr2:18626377-18626781 FORWARD LENGTH=134	23	14459	1	1
	AT5G58870.1	| Symbols: ftsh9 | FTSH protease 9 | chr5:23770080-23773719 REVERSE LENGTH=806	21	88012	1	1
	AT1G49750.1	| Symbols: | Leucine-rich repeat (LRR) family protein | chr1:18411177-18412779 REVERSE LENGTH=494	21	55171	1	1
	AT5G43390.1	| Symbols: | Uncharacterised conserved protein UCP015417, vWA | chr5:17422940-17424871 REVERSE LENGTH=643	19	73346	1	1
Mitochondria	AT5G58270.1	| Symbols: STA1, ATATM3, ATM3 | ABC transporter of the mitochondrion 3 | chr5:23562168-23567040 FORWARD LENGTH=728	26	80598	1	1
	AT1G19140.1	| Symbols: | FUNCTIONS IN: molecular_function unknown; INVOLVED IN: ubiquinone biosynthetic process; LOCATED IN: mitochondrion; EXPRESSED IN: 24 plant structures; EXPRESSED DURING: 15 growth stages; CONTAINS InterPro DOMAIN/s: COQ9 (InterPro:IPR013	23	34433	1	1
Peroxisome	AT1G20620.1	| Symbols: CAT3, SEN2, ATCAT3 | catalase 3 | chr1:7143142-7146193 FORWARD LENGTH=492	283	57059	15	10
	AT4G35090.1	| Symbols: CAT2 | catalase 2 | chr4:16700937-16703215 REVERSE LENGTH=492	167	57237	12	5
	AT1G20630.1	| Symbols: CAT1 | catalase 1 | chr1:7146812-7149609 FORWARD LENGTH=492	155	57068	8	5
	AT3G14415.1	| Symbols: | Aldolase-type TIM barrel family protein | chr3:4818667-4820748 FORWARD LENGTH=367(GO)	63	40338	6	1
	AT1G68010.1	| Symbols: HPR, ATHPR1 | hydroxypyruvate reductase | chr1:25493418-25495720 FORWARD LENGTH=386	41	42449	1	1
	AT5G09660.1	| Symbols: PMDH2 | peroxisomal NAD-malate dehydrogenase 2 | chr5:2993645-2995551 REVERSE LENGTH=354	35	37688	3	2
	AT2G22780.1	| Symbols: PMDH1 | peroxisomal NAD-malate dehydrogenase 1 | chr2:9689995-9691923 REVERSE LENGTH=354	23	37841	2	1
	AT2G13360.1	| Symbols: AGT, AGT1, SGAT | alanine:glyoxylate aminotransferase | chr2:5539417-5540902 REVERSE LENGTH=401	22	44465	1	1

Supplementary Table 3.
Number of peroxisomes targeted by ATG18a-GFP or GFP-2×FYVE

ATG18a-GFP			
	Peroxisome	Other	Total
Wild type	7	2	9
peup1	84	26	109
peup4	76	21	97

GFP-2×FYVE			
	Peroxisome	Other	Total
Wild type	5	8	13
peup1	133	80	213
peup4	269	307	576

Supplementary Table 4.

Statistical analysis of ATG18a-GFP and GFP-2x×FYVE targeting to peroxisome aggregates in wild type, *peup1*, and *peup2* under normal light (100 μmol $m^{-2}s^{-1}$) and high-intensity light (1000 μmol $m^{-2}s^{-1}$). **a,** Total number of peroxisome aggregates (a), peroxisome aggregates with micro pexophagosome (b), autophagosome-like structure targeted by ATG18a-GFP (upper) or GFP-2xFYVE (lower) (c), and tested cells (d) were counted in wild type, *peup1*, and *peup4* expressing *RFP-PTS1* and *ATG18a-GFP* (upper) or *GFP-2xFYVE* (lower) under low- or high-intensity light. The (e), (f), and (g) are the ratio of (b) to (a), (b) to (c), and (b) to (d), respectively. SD in parenthesis means standard deviation.

ATG18-GFP

Light intensity		a	b	c	d	e (SD)	f (SD)	g (SD)
100 μmol $m^{-2}s^{-1}$	Wild type	1	0	2	121	0.00	0.00	0.00
	peup1	102	1	2	162	0.01 (0.03)	0.10 (0.32)	0.03 (0.03)
	peup4	102	26	44	213	0.24 (0.13)	0.54 (0.22)	0.12 (0.07)
1000 μmol $m^{-2}s^{-1}$	Wild type	19	8	19	148	0.43 (0.39)	0.46 (0.30)	0.07 (0.07)
	peup1	66	15	18	151	0.23 (0.14)	0.83 (0.24)	0.11 (0.08)
	peup4	97	58	91	154	0.62 (0.17)	0.63 (0.17)	0.43 (0.18)

GFP-2xFYVE

		a	b	c	d	e (SD)	f (SD)	g (SD)
100 μmol $m^{-2}s^{-1}$	Wild type	10	0	1	225	0.00	ND	0.00
	peup1	95	0	0	119	0.00	ND	0.00
	peup4	49	0	0	142	0.00	ND	0.00
1000 μmol $m^{-2}s^{-1}$	Wild type	9	1	2	155	ND	ND	ND
	peup1	103	2	3	135	0.02 (0.05)	0.67 (0.58)	0.02 (0.04)
	peup4	108	10	17	193	0.12 (0.10)	0.81 (0.75)	0.07 (0.06)

Supplementary Table 5.

Statistical analysis of cells containing peroxisomes targeted by ATG18a-GFP in light. Total number of cells targeted by ATG18a-GFP was counted in wild type, *peup1*, and *peup4* expressing *RFP-PTS1* and *ATG18a-GFP* under normal light (100 μmol $m^{-2}s^{-1}$) and high-intensity light (1000 μmol $m^{-2}s^{-1}$). SD in parenthesis means standard deviation.

Ratio of cell harboring ATG18a-GFP-targeted peroxisomes

Light intensity	Wild type (SD)	*peup1* (SD)	*peup4* (SD)
100 μmol $m^{-2}s^{-1}$	0.144 (0.09)	0.64 (0.10)	0.53 (0.07)
1000 μmol $m^{-2}s^{-1}$	0.761 (0.16)	0.92 (0.11)	0.88 (0.07)

Supplementary Table 6.

Statistical analysis of Venus-Vam3 targeting to peroxisomes in wild type, *peup1*, and *peup2* in light. Total number of peroxisomes aggregates (a), peroxisome aggregates with micro pexophagosome (b), autophagosome-like structure targeted by Venus-VAM3 (c), and tested cells (d) were counted in wild type, *peup1*, and *peup4* expressing *Venus-VAM3* and *RFP-PTS1* under normal light (100 μmol $m^{-2}s^{-1}$) and high-intensity light (1000 μmol $m^{-2}s^{-1}$). The (e), (f), and (g) are the ratio of (b) to (a), (b) to (c), and (b) to (d), respectively. SD in parenthesis means standard deviation.

Venus-Vam3 (100 μmol $m^{-2}s^{-1}$)

	a	b	c	d	e (SD)	f (SD)	g (SD)
Wild type	9	3	7	314	0.31 (0.46)	0.50 (0.55)	0.01 (0.02)
peup1	340	11	20	311	0.03 (0.30)	ND	0.03 (0.03)
peup4	86	29	51	289	0.37 (0.13)	0.55 (0.12)	0.10 (0.05)

Venus-Vam3 (1000 μmol $m^{-2}s^{-1}$)

	a	b	c	d	e (SD)	f (SD)	g (SD)
Wild type	18	11	14	318	0.36 (0.45)	0 (0)	0.03 (0.06)
peup1	170	3	3	204	0.02 (0.04)	ND	0.01 (0.02)
peup4	122	66	91	180	0.54 (0.09)	0.71 (0.18)	0.35 (0.12)

Supplementary Video Legend

Supplementary Video 1. Wild type in light.

Time-lapse images of peroxisomes (GFP-PTS1, green) and chloroplasts (autofluorescence, magenta) in wild type obtained every 5 s for 250 s using CLSM. Images are stacked at 5 frames per second. Scale bar, 10 μm.

Supplementary Video 2. The *peup1* mutant in light.

Time-lapse images of peroxisomes (GFP-PTS1, green) and chloroplasts (autofluorescence, magenta) in *peup1* obtained every 5 s for 250 s using CLSM. Images are stacked at 5 frames per second. Large peroxisome aggregates are formed continuously. Scale bar, 10 μm.

Supplementary Video 3. *The peup4* mutant in light.

Time-lapse images of peroxisomes (GFP-PTS1, green) and chloroplasts (autofluorescence, magenta) in *peup4* obtained every 5 s for 250 s using CLSM. Images are stacked at 5 frames per second. Peroxisome aggregates are occasionally formed in the cells. Scale bar, 10 μm.

Supplementary Video 4. Peroxule formation in *peup4* in light

Time-lapse images of peroxules (GFP-PTS1, green) and chloroplasts (autofluorescence, magenta) in *peup4* obtained every 5 s for 250 s using CLSM. Images are stacked at 5 frames per second. Scale bar, 10 μm. Peroxules are formed in the peroxisome aggregates in *peup4*.

Supplementary Video 5. ATG18a-GFP in wild type.

Time-lapse images of peroxisomes (RFP-PTS1, magenta) and ATG18a-GFP (green) in a wild-type cell obtained every 5 s for 200 s using CLSM. Images are stacked at 5 frames per second. The peroxisome is gradually surrounded by ATG18a-GFP and transported to an undefined structure. Scale bar, 10 μm.

Supplementary Video 6. ATG18a-GFP in *peup1.*

Time-lapse images of peroxisomes (RFP-PTS1, magenta) and ATG18a-GFP (green) in a *peup1* cell obtained every 5 s for 200 s using CLSM. Images are stacked at 5 frames per second. The peroxisome aggregate is targeted, but not surrounded, by ATG18a-GFP. Scale bar, 10 μm.

Supplementary Video 7. ATG18a-GFP in *peup4.*

Time-lapse images of peroxisomes (RFP-PTS1, magenta) and ATG18a-GFP (green) in a *peup4* cell obtained every 5 s for 200 s using CLSM. Images are stacked to 5 frames per second. The peroxisome aggregate surrounded by ATG18a-GFP moves in a cell. Scale bar, 10 μm.

Supplementary Video 8. FRAP analysis.

Time-lapse images of FRAP analysis of peroxisome aggregation (RFP-PTS1, magenta) targeted by ATG18-GFP (green) in *peup1* were obtained using CLSM every 1 s for 60 s from before photobleaching to after fluorescence recovery. Photobleaching was performed at the spots indicated by white circle. Scale bar, 10 μm.

Supplementary Video 9. GFP-2×FYVE in wild type.

Time-lapse images of peroxisome (RFP-PTS1, magenta) and GFP-2×FYVE (green) in a wild-type cell obtained every 5 s for 200 s using CLSM. Images are stacked at 5 frames per second. The peroxisome is gradually surrounded by GFP-2×FYVE. Scale bar, 10 μm.

Supplementary Video 10. GFP-2×FYVE in *peup4*.

Time-lapse image of peroxisome (RFP-PTS1, magenta) and GFP-2×FYVE (green) in a *peup4* cell obtained every 5 s for 200 s using CLSM. Images are stacked to 5 frames per second. The peroxisome aggregate surrounded by GFP-2×FYVE moves in a cell. Scale bar, 5 μm.

Supplementary Video 11. The bulb structures in wild type.

Time-lapse images of peroxisomes (RFP-PTS1, magenta) and vacuolar membranes (Venus-VAM3, green) in wild type were obtained using CLSM every 5 s for 250 s. Peroxisomes are surrounded by vacuolar structures similar to bulbs. Scale bar, 10 μm.

Supplementary Video 12. The bulb structures in *peup4*.

Time-lapse images of peroxisomes (RFP-PTS1, magenta) and vacuolar membranes (Venus-VAM3, green) in *peup4* were obtained using CLSM every 5 s for 250 s. Peroxisomes are surrounded by vacuolar structures similar to bulbs. Scale bar, 5 μm.